Electronic Supplementary Information

# New AIE-active dinuclear Ir(III) complexes with reversible piezochromic phosphorescence behaviour†

**Guangfu Li[a], Xinyao Ren[a], Guogang Shan[a], Weilong Che[a], Dongxia Zhu*[a], Likai Yan[a], Zhongmin Su*[a], Martin R. Bryce*[b]**

[a]*Institute of Functional Material Chemistry, Faculty of Chemistry, Northeast Normal University, Changchun 130024, People's Repubic of China; Fax: +86-0431-85684009*

*Tel.: +86-431-85099108, E-mail: zhudx047@nenu.edu.cn; zmsu@nenu.edu.cn*

[b] *Department of Chemistry, Durham University, Durham, DH1 3LE, UK*

*E-mail: m.r.bryce@durham.ac.uk*

## Table of Contents



.

## 1. Experimental - general information

Materials obtained from commercial suppliers were used without further purification unless otherwise stated. All glassware, syringes, magnetic stirring bars, and needles were thoroughly dried in a convection oven. Reactions were monitored using thin layer chromatography (TLC). Commercial TLC plates were used and the spots were visualised under UV light at 254 and 365 nm. $^{1}$H NMR, $^{13}$C NMR and 2D $^{1}$H NMR spectra were recorded at 25 ºC on a Varian 500 MHz spectrometer, $^{13}$C NMR spectra were recorded at 25 ºC on a Varian 125 MHz, with TMS as internal standard. The chemical shifts (δ) are given in parts per million relative to internal standard TMS (0 ppm for $^{1}$H) and DMSO-$d_6$ (40.0 ppm for $^{13}$C). The molecular weights of the complexes were obtained by using matrix-assisted laser desorption-ionization time-of-flight (MALDI-TOF) mass spectrometry. Elemental analysis was obtained using a Flash EA1112 analyser. Powder X-ray diffraction (XRD) patterns of the samples were collected on a Rigaku Dmax 2000. Differential scanning calorimetry (DSC) curves were obtained with a Perkin-Elmer thermal analysis DSC-7 under nitrogen with a heating rate 10 °C min$^{-1}$. Transmission electron microscopy (TEM) and electron diffraction pattern of the sample were performed using a TECNAI F20 microscope. The samples were prepared by placing microdrops of the solution on a holey carbon copper grid. UV-vis absorption spectra were recorded on a Shimadzu UV-3100 spectrophotometer. Photoluminescence spectra were collected on a Shimadzu RF-5301pc spectrophotometer and Maya 2000Pro optical fiber spectrophotometer. PL efficiencies were measured with an integrating sphere (C-701, Labsphere Inc.) with a 365 nm Ocean Optics LLS-LED as the excitation source, and the laser was introduced into the sphere through the optical fiber. The excited-state lifetimes were measured by exciting the samples with 355 nm light pulses with ~3 ns pulse width from a Quanty-Ray DCR-2 pulsed Nd: YAG laser. For the crystal structure of complex **1**, the data were collected on a Bruker Smart Apex II CCD diffractometer with graphite-monochromated Mo Kα radiation ($\lambda$ = 0.71073 Å) at room temperature.

**Complexes 1 and 2 - synthesis and characterisation**

**Synthesis of $[(2F\text{-}ppz)_2Ir\text{-}(L)\text{-}Ir(2F\text{-}ppz)_2]\ [PF_6]_2$ (complex 1)**

A yellow suspension of the dichloro-bridged diiridium complex $[Ir(2Cl\text{-}ppz)_2Cl]_2$[1] (0.100 g, 0.1 mmol, 1.00 eq.) and bridging ligand (L) (0.029 g, 0.1 mmol, 1.00 eq.) in MeOH (15 mL) and $CH_2Cl_2$ (15 mL) was refluxed under an inert atmosphere of $N_2$ in the dark for 4 h. The orange solution was then cooled to room temperature, and solid ammonium hexafluorophosphate (0.037 g, 0.2 mmol, 2.00 eq.) was added to the solution. The mixture was stirred for 45 min at room temperature and the suspension was then filtered and the precipitate was washed with petroleum ether and dried. The crude product was recrystallised from petroleum ether to yield complex **1** as an orange solid (0.141 g, 84% yield). Complex **1** exists in solution as a pair of diastereoisomers. There is a slight excess of one isomer over the other (ca. 1.23:1). The major isomer is arbitrarily designated as α; the minor as β. Where separate signals are visible for the two isomers, they are reported separately, but in each case integrals are quoted relative to the molecular formula for that isomer (i.e. 1H represents one hydrogen for that isomer). $^1$H NMR (500 MHz, DMSO-$d_6$, δ [ppm]): 9.33 (s, 1H, $H^{a\beta}$), 9.31 (s, 1H, $H^{a\alpha}$), 9.30 (d, *J* = 5.0 Hz, 1H, $H^{E6\beta}$), 9.29 (d, *J* = 6.0 Hz, 1H, $H^{E6\alpha}$), 9.17 (d, 1H, *J* = 6.0 Hz, $H^{B3\beta}$), 9.16 (d, *J* = 5.0 Hz,1H, $H^{B3\alpha}$), 8.51 (d, *J* = 9.0 Hz, 2H, $H^{E3\alpha+\beta}$), 8.35 (t, *J* = 8.0 Hz, 2H, $H^{E4\alpha+\beta}$), 8.01 (d, *J* = 7.0 Hz, 2H, $H^{D3\alpha+\beta}$), 7.88 (d, *J* = 5.0 Hz, 1H, $H^{B5\alpha}$), 7.80-7.76 (m, 3H, $H^{B5\beta+D5\alpha+\beta}$), 7.58 (s, 1H, $H^{A4\beta}$), 7.51 (s, 1H, $H^{A4\alpha}$), 7.35 (s, 1H, $H^{A6\alpha}$), 7.28 (s, 1H, $H^{A6\beta}$), 7.27 (s, 1H, $H^{C6\beta}$), 7.23 (s, 1H, $H^{C6\alpha}$), 7.04 (t, *J* = 6.0 Hz, 1H, $H^{B4\alpha}$), 7.01 (t, *J* = 6.0 Hz, 1H, $H^{B4\beta}$), 6.98 (t, *J* = 6.0 Hz, 1H, $H^{D4\beta}$), 6.91 (t, *J* = 6.0 Hz, 1H, $H^{D4\alpha}$), 6.71 (d, *J* = 5.0 Hz, 4H, $H^{F2\alpha+\beta}$), 5.89 (s, 1H, $H^{C4\alpha}$), 5.79 (s, 1H, $H^{C4\beta}$), 5.63 (t, *J* = 5.0 Hz, 2H, $H^{E5\alpha+\beta}$). $^{13}$C NMR (DMSO-$d_6$, 125 MHz, δ[ppm]): 109.9($C^{D4\alpha+\beta}$), 110.1($C^{B4\alpha+\beta}$), 117.7($C^{C1\alpha+\beta}$), 118.1($C^{A1\alpha+\beta}$), 123.0($C^{F2\alpha+\beta}$), 125.1($C^{A6\alpha+\beta}$), 125.9($C^{C6\alpha+\beta}$), 130.3($C^{C5\alpha+\beta}$), 130.5($C^{A5\alpha}$), 130.6($C^{C4\beta}$), 130.8($C^{C4\alpha}$), 130.9($C^{E5\alpha+\beta}$), 131.0($C^{A5\beta}$), 131.3($C^{D5\alpha+\beta}$), 131.9($C^{E3\alpha+\beta}$), 134.0($C^{B3\alpha+\beta}$),

134.2($C^{E6\alpha+\beta}$), 136.5($C^{A3\alpha+\beta}$), 138.0($C^{C3\alpha+\beta}$), 138.2($C^{F1\alpha+\beta}$), 138.4($C^{E2\alpha}$), 138.6($C^{E2\beta}$), 140.8($C^{E4\alpha+\beta}$), 141.2($C^{B5\beta}$), 141.3($C^{A4\alpha}$), 141.5($C^{A4\beta}$), 141.7($C^{B5\alpha}$), 147.7($C^{C2\alpha}$), 147.8($C^{C2\beta}$), 151.5($C^{D3\alpha}$), 151.6($C^{D3\beta}$), 155.6($C^{A2\alpha}$), 155.7($C^{A2\beta}$), 172.4($C^{a\alpha}$), 172.5($C^{a\beta}$). MS: (MALDI-TOF) [m/z]: 1676.14 (M-$PF_6$) (calcd: 1677.28). Anal. Calcd. for $C_{54}H_{34}F_{20}Ir_2N_{12}P_2$: C 38.67, H 2.04, N 10.02. Found C 38.84, H 2.01, N 9.98. Crystals for X-ray analysis were obtained by the slow diffusion of ether vapor into a solution of the complex in acetonitrile solution, with slow evaporation of the solution.

**Synthesis of [(2F-ppz)$_2$Ir-(L2)-Ir(2F-ppz)$_2$] [$PF_6$]$_2$ (complex 2)**

The synthesis of complex **2** was similar to that of complex **1** except that the ancillary ligand **L1** was replaced by **L2**. Complex **2** was obtained as a red solid (0.141 g, 80% yield). $^1$H NMR (500 MHz, DMSO-$d_6$, δ [ppm]): 9.52 (s, 1H, $H^a$), 9.30 (d, *J* = 3.0 Hz, 1H, $H^{E6}$), 9.14 (d, *J* = 3.0 Hz, 1H, $H^{D3}$), 8.53 (d, *J* = 8.0 Hz, 1H, $H^{B3}$), 8.36 (t, *J* = 8.0 Hz, 1H, $H^{E4}$), 8.20 (d, *J* = 5.0 Hz, 1H, $H^{D5}$), 8.05 (d, *J* = 5.5 Hz, 1H, $H^{B5}$), 7.79 (t, *J* = 7.0 Hz, 1H, $H^{E5}$), 7.61 (s, 1H, $H^{C4}$), 7.36 (d, *J* = 8.0 Hz, 2H, $H^{F3}$), 7.23 (d, *J* = 8.0 Hz, 1H, $H^{E3}$), 6.96 (m, 3H, $H^{A4+D4+C6}$), 6.81 (d, *J* = 7.0 Hz, 2H, $H^{F2}$), 5.94 (s, 1H, $H^{A6}$), 5.67 (t, *J* = 7.5 Hz, 1H, $H^{B4}$). $^{13}$C NMR (DMSO-$d_6$, 125 MHz, δ[ppm]): 109.9($C^{D4}$), 110.0($C^{C6}$), 117.4($C^{C1}$), 118.1($C^{A1}$), 122.7($C^{F2}$), 124.6($C^{A6}$), 125.7($C^{E3}$), 127.0($C^{F3}$), 131.0($C^{A4}$), 131.0($C^{B4}$), 131.1($C^{E5}$), 131.5($C^{B3}$), 134.0($C^{D3}$), 134.2($C^{E6}$), 137.1($C^{F4}$), 138.0($C^{F1}$), 138.3($C^{C3}$), 138.5($C^{A3}$), 138.6($C^{C5}$), 138.8($C^{A5}$), 138.9($C^{E2}$), 140.9($C^{E4}$), 141.2($C^{C4}$), 141.9($C^{D5}$), 147.3($C^{C2}$), 151.7($C^{B5}$), 155.9($C^{A2}$), 171.7($C^a$). MS: (MALDI-TOF) [m/z]: 1754.18 (M-$PF_6$) (calcd: 1753.37). Anal. Calcd. for $C_{60}H_{38}F_{20}Ir_2N_{12}P_2$: C 41.10, H 2.18, N 9.59. Found C 41.11, H 2.22, N 9.62.

## 2. Photophysical properties

**Table S1** Photophysical and electrochemical characteristics of complexes **1** and **2**.

| | Absorption and emission at room temperature | | | Emission at 77 K | Electrochemical Data[d] | | $K_r \times 10^6$ $s^{-1}$ | $K_{nr} \times 10^6$ $s^{-1}$ |
|---|---|---|---|---|---|---|---|---|
| | $\lambda_{abs}$[a](nm) | $\lambda_{em}$[b](nm) | $\Phi_{em}$[b]($\tau$[b][μs]) | $\lambda_{em}$[c](nm) | $E_{ox}^{1/2}$(V) | $E_{red}^{1/2}$(V) | | |
| **1** | 249(0.844),319$_{sh}$(0.310),357$_{sh}$(0.235) | 612 | 0.31(0.18) | 560 | 0.69 | -1.48 | 1.72 | 3.83 |
| **2** | 253(0.674),322$_{sh}$(0.192),366$_{sh}$(0.203) | 627 | 0.24(0.17) | 572 | 0.65 | -1.47 | 1.41 | 4.47 |

[a]Measured in $CH_2Cl_2$ ($1.0\times10^{-5}$ M). [b]Measured in solid state ($\lambda_{exc}$ = 365 nm; error for $\Phi_L$ ± 5%). [c]In $CH_3CN$ glass. [d]The data were versus Fc+/Fc (Fc is ferrocene).

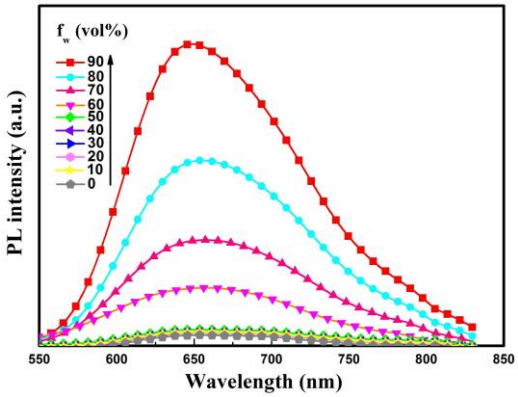


**Fig. S1** Emission spectra of complex **2** in $CH_3CN$–water mixtures with different water fractions (0–90%, v/v) at room temperature.

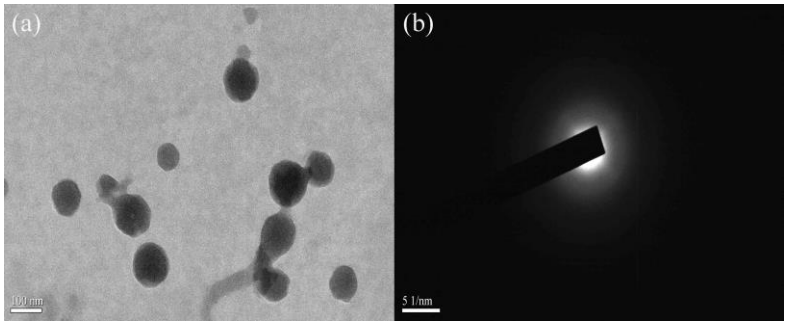


**Fig. S2** (a) TEM image of nanoaggregates of complex **1** formed in $CH_3CN$–$H_2O$ mixtures with 90% water fraction. (b) Electron diffraction pattern of the amorphous nanoaggregates.

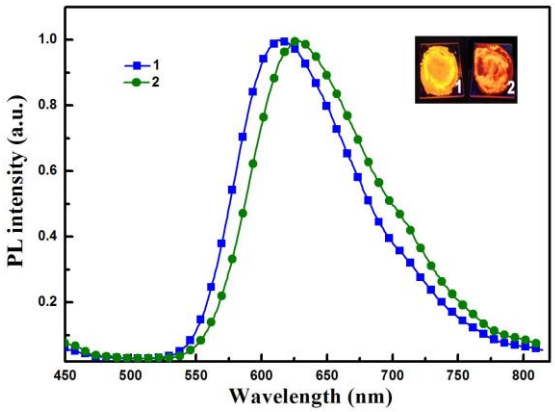


**Fig. S3** Emission spectra of complexes **1** and **2** in solid film state at room temperature.

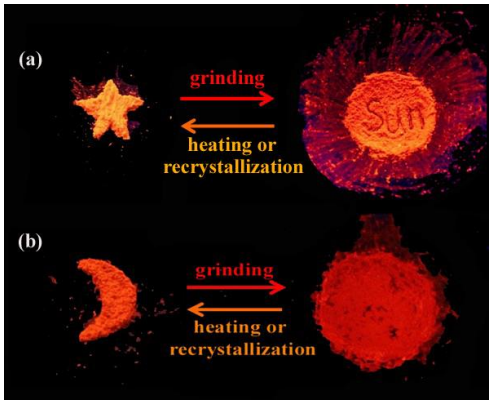


**Fig. S4** Emission colour upon irradiation by UV-light of **P1** and **G1** (a); and **P2** and **G2** (b).

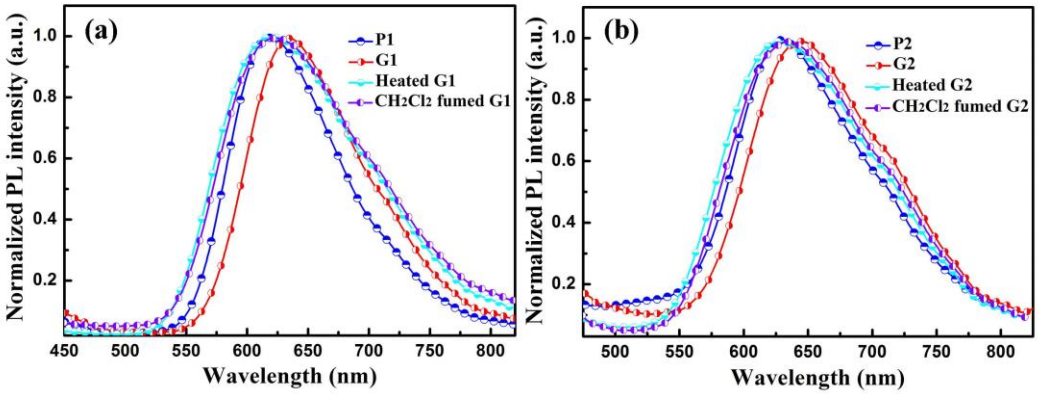


**Fig. S5** The emission spectra of unground, ground samples, heated ground samples, and ground samples exposed to $CH_2Cl_2$ vapour, corresponding to **P1**, **G1**, Heated **G1** and **G1** exposed to $CH_2Cl_2$ vapour, respectively (a); and **P2** and **G2** (b).

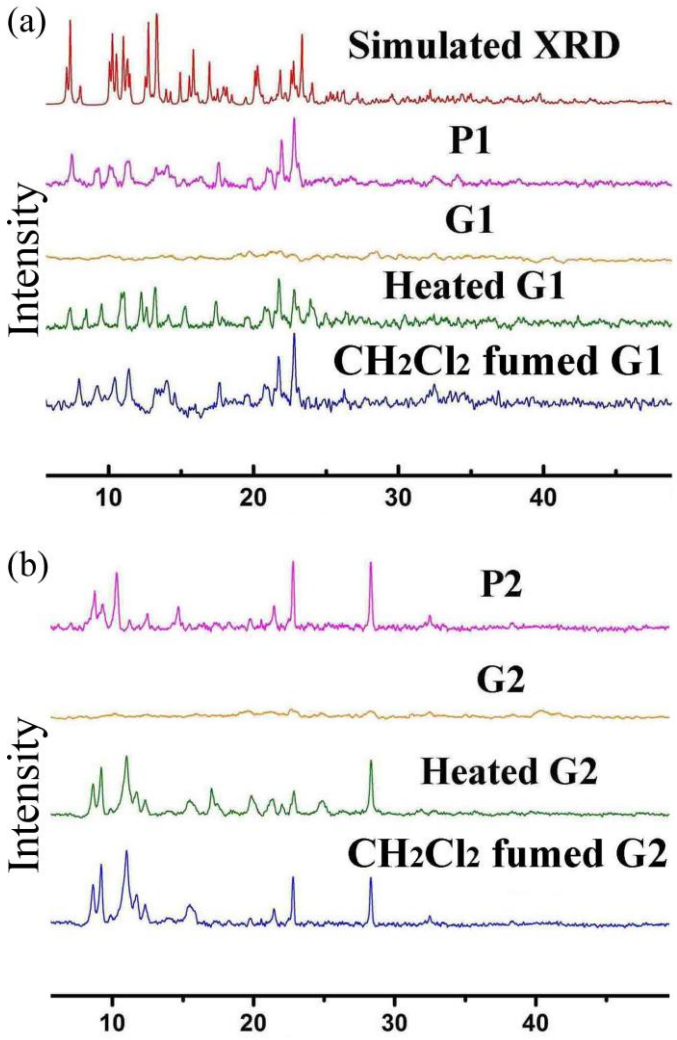


**Fig. S6** Expansion of the powder X-ray diffraction patterns shown in Figure 5 of the manuscript: (a) and (b) of the corresponding samples.

**Table S2** The excited-state lifetimes ($\tau$) in various states of complexes **1** and **2**.

| | As-synthesized | Ground | Heated | $CH_2Cl_2$ fumed |
|---|---|---|---|---|
| **1** | 0.18 μs | 0.22 μs | 0.17 μs | 0.18 μs |
| **2** | 0.17 μs | 0.20 μs | 0.17 μs | 0.18 μs |

## 3. Quantum chemical calculations

All calculations were performed with Gaussian 09 program package.[2] The B3LYP functional was employed for all DFT calculations. The 6-31G* basis set was employed for H, C, N, F atoms, while the iridium atom was described by the Hay-Wadt effective core potential (ECP) and a double-ξ basis set LANL2DZ. The calculations on frontier molecular orbital (FMO) properties in the ground state ($S_0$) of complex **1** were carried out in solution and solid state, respectively. The properties of the solution state were calculated after optimization in the solvent. The solvent effect was taken into account by using the polarisable continuum model (PCM) with acetonitrile as solvent. Moreover, the calculations of the solid state structure were performed using the experimental crystal structure data of complex **1**.

**Table S3** Selected calculated bond lengths (Å), bond angles (°) and dihedral angles (°) at both optimized $S_0$ and $T_1$ geometries for complex **1** in acetonitrile solution.

| | $S_0$ | $T_1$ |
|---|---|---|
| Ir1-N1 | 2.057 | 2.053 |
| Ir1-C1 | 2.027 | 2.029 |
| Ir1-C2 | 2.031 | 2.025 |
| Ir1-N2 | 2.051 | 2.049 |
| Ir1-N3 | 2.204 | 2.213 |
| Ir1-N4 | 2.234 | 2.205 |
| Ir2-N5 | 2.057 | 2.054 |
| Ir2-C3 | 2.027 | 2.024 |
| Ir2-C4 | 2.031 | 2.033 |
| Ir2-N6 | 2.051 | 2.055 |
| Ir2-N7 | 2.204 | 2.199 |
| Ir2-N8 | 2.234 | 2.258 |
| C1-Ir1-C2 | 88.17 | 87.65 |
| C1-Ir1-N2 | 95.16 | 94.57 |
| C2-Ir1-N3 | 173.59 | 177.99 |
| N3-Ir1-N2 | 96.00 | 98.31 |
| C1-Ir1-N4 | 171.88 | 168.07 |
| N3-Ir1-N4 | 75.26 | 76.35 |
| C1-Ir1-N3 | 97.02 | 91.76 |
| N4-Ir1-C2 | 99.70 | 104.26 |

| | | |
|---|---|---|
| N1-Ir1-N2 | 173.37 | 173.38 |
| C3-Ir2-C4 | 88.17 | 87.18 |
| C3-Ir2-N6 | 95.16 | 95.72 |
| C4-Ir2-N7 | 173.59 | 174.73 |
| N7-Ir2-N6 | 96.00 | 95.97 |
| C3-Ir2-N8 | 171.88 | 171.27 |
| N7-Ir2-N8 | 75.26 | 75.28 |
| C3-Ir2-N7 | 97.02 | 96.29 |
| N8-Ir2-C4 | 99.70 | 101.40 |
| N5-Ir2-N6 | 173.37 | 173.59 |
| C5-N4-C6-C7 | 46.10 | 19.78 |
| C8-N8-C9-C10 | 134.22 | 143.92 |

## 4. $^{1}$H NMR, 2D NMR spectra of complexes 1 and 2 at room temperature

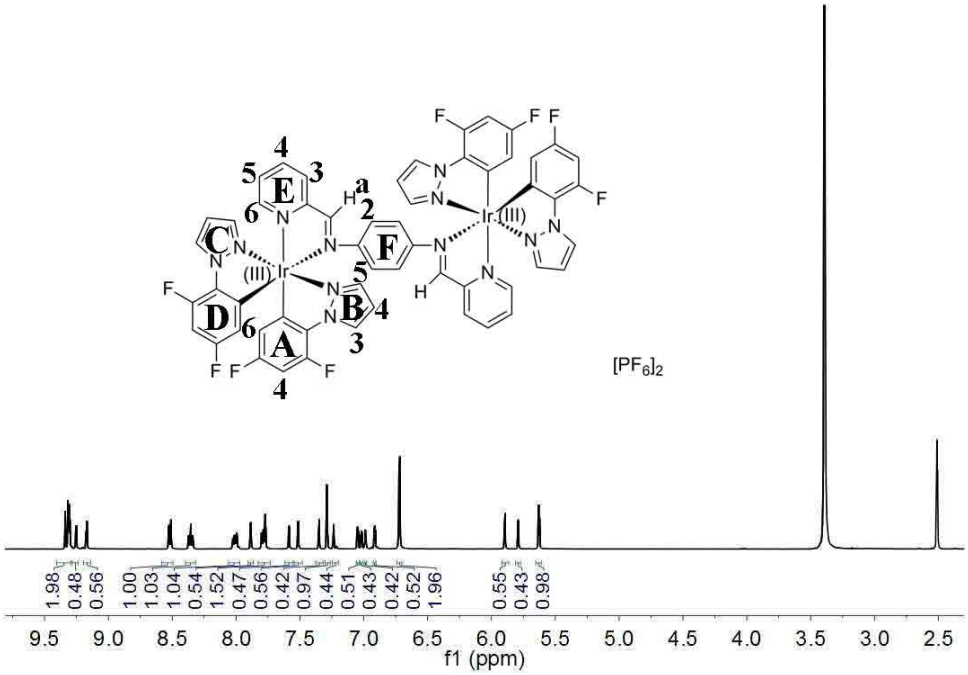


**Fig. S7** $^{1}$H NMR spectrum of complex **1** in DMSO-$d_6$.

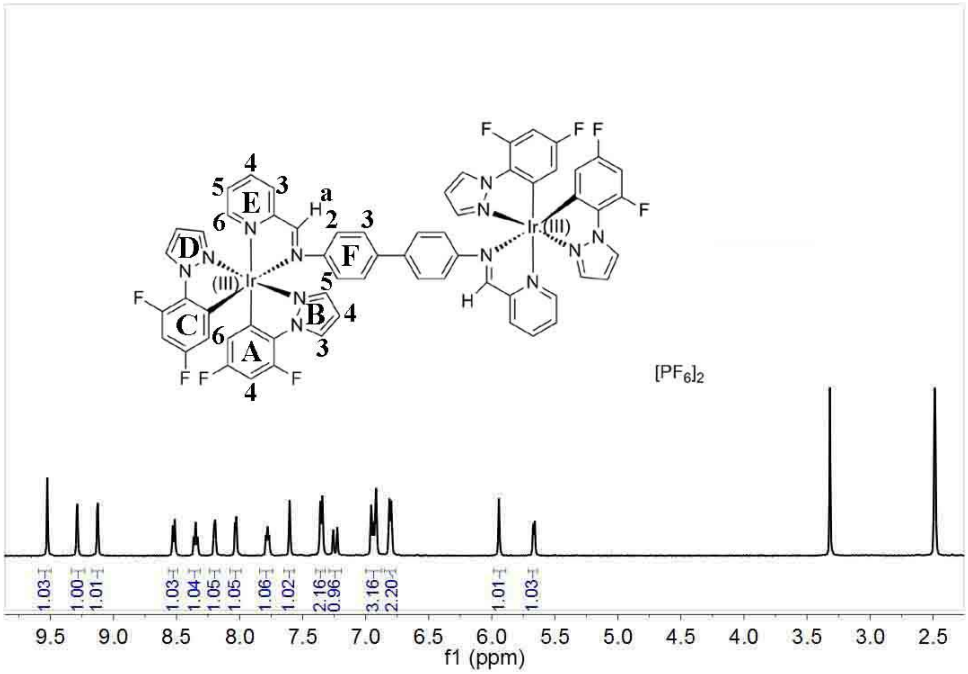


**Fig. S8** $^{1}$H NMR spectrum of complex **2** in DMSO-$d_6$.

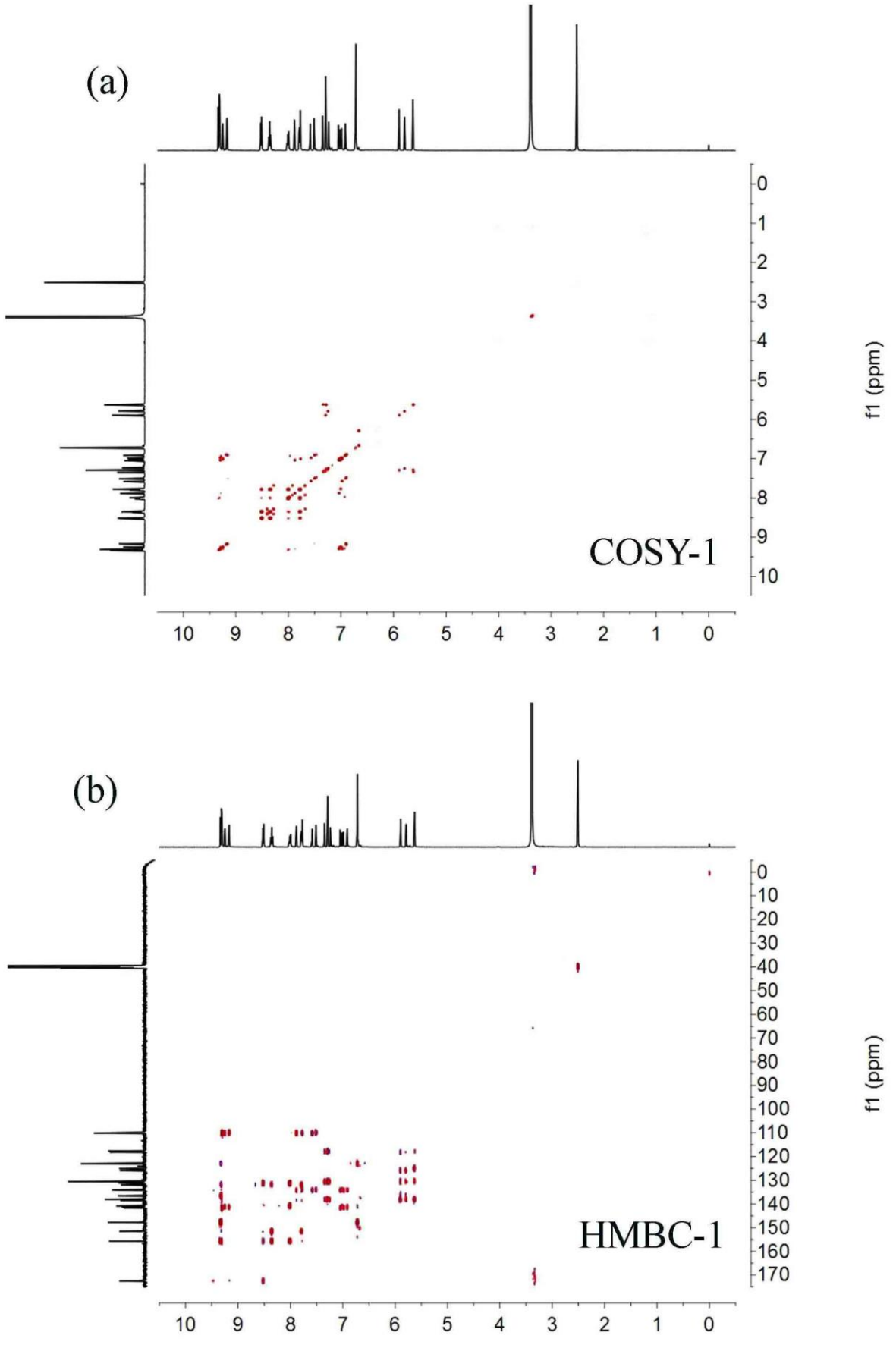
(a)
COSY-1
f1 (ppm)
(b)
HMBC-1
f1 (ppm)

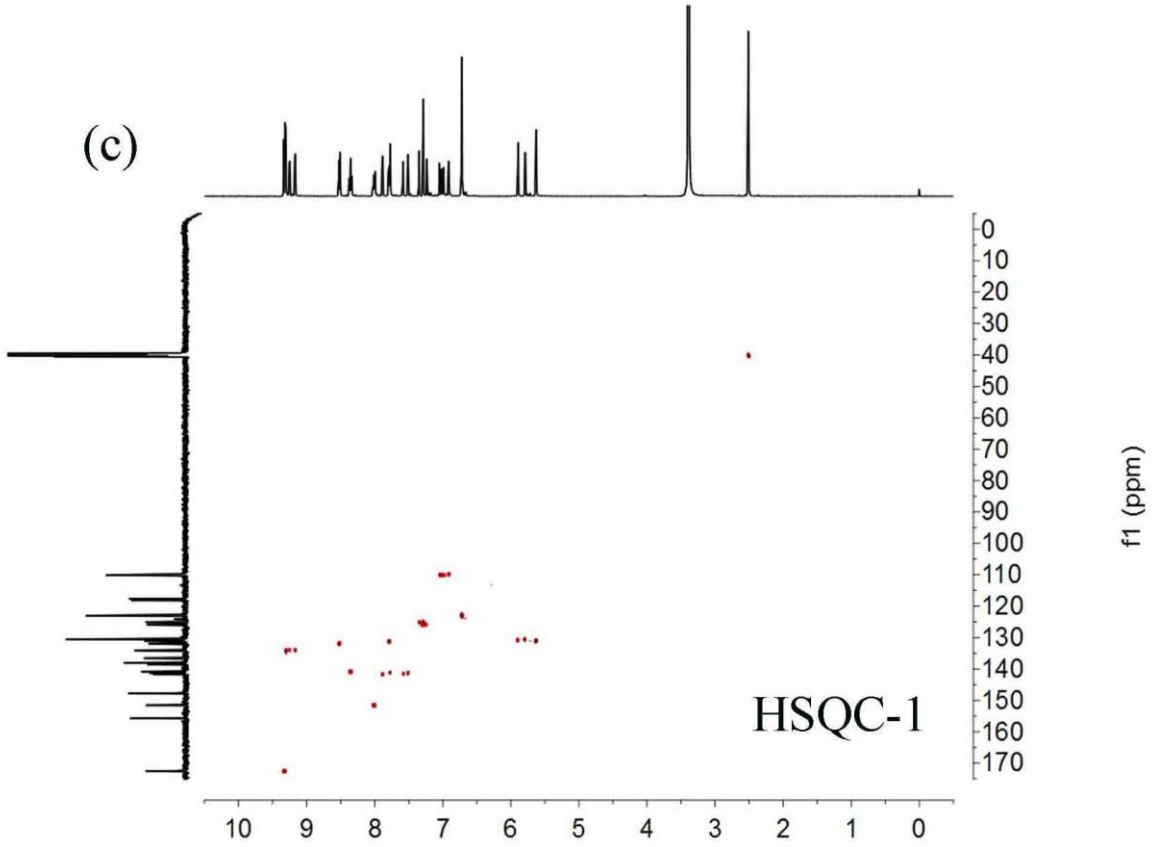


**Fig. S9** (a) 2D COSY NMR spectrum of complex **1** in DMSO-$d_6$. (b) 2D HM BC NMR spectrum of complex **1** in DMSO-$d_6$. (c) 2D HSQC NMR spectrum of complex **1** in DMSO-$d_6$.

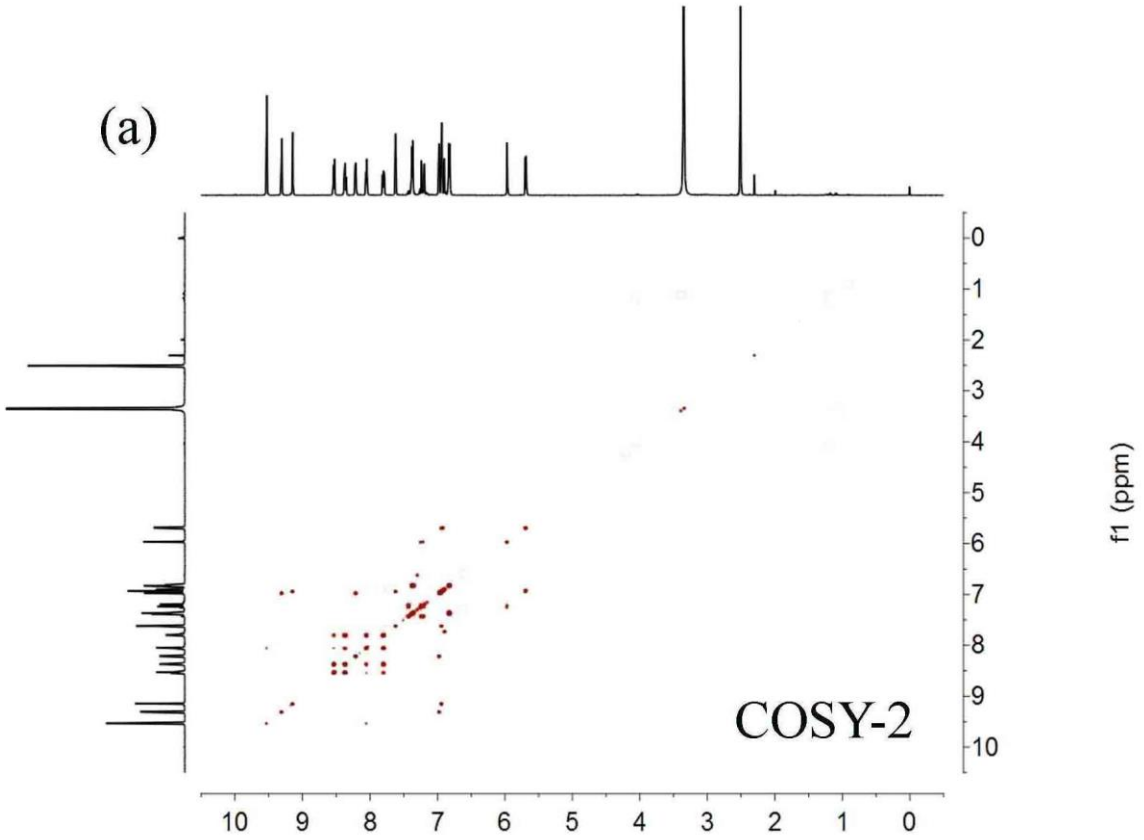
(a)
COSY-2
f1 (ppm)
0
1
2
3
4
5
6
7
8
9
10
10 9 8 7 6 5 4 3 2 1 0

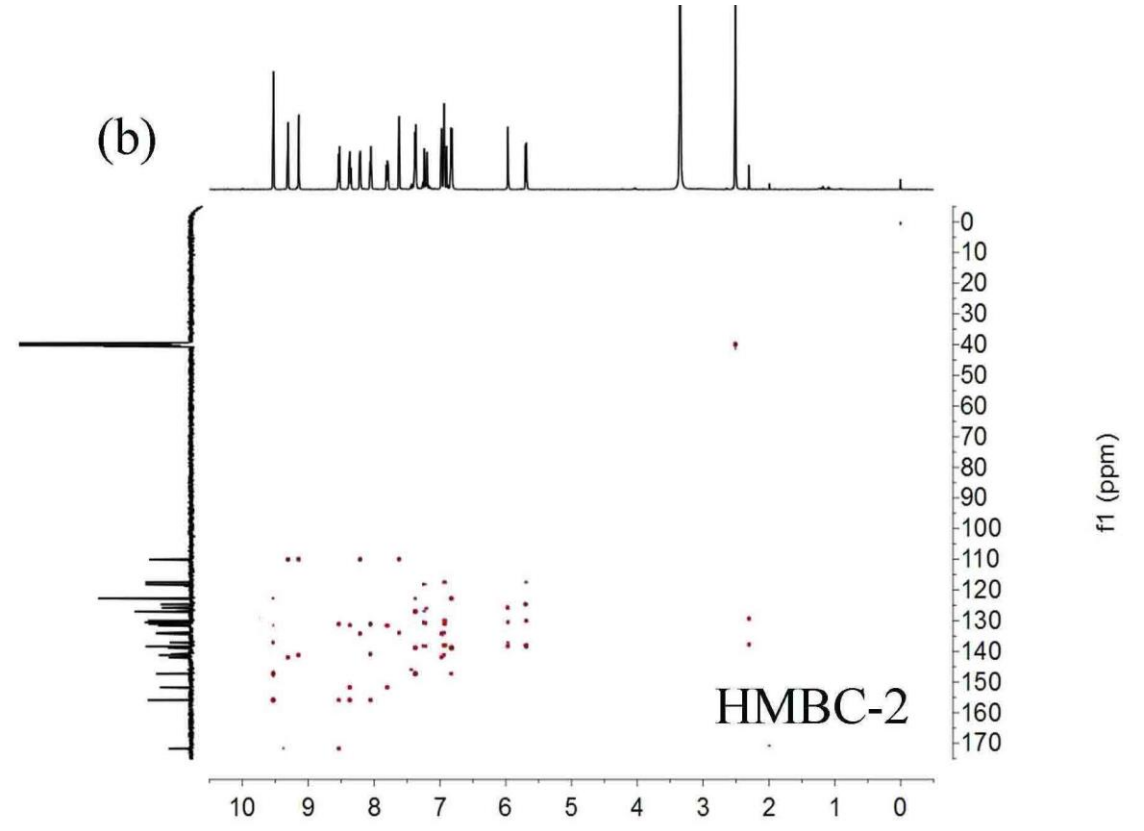
(b)
HMBC-2
f1 (ppm)
0
10
20
30
40
50
60
70
80
90
100
110
120
130
140
150
160
170
10 9 8 7 6 5 4 3 2 1 0

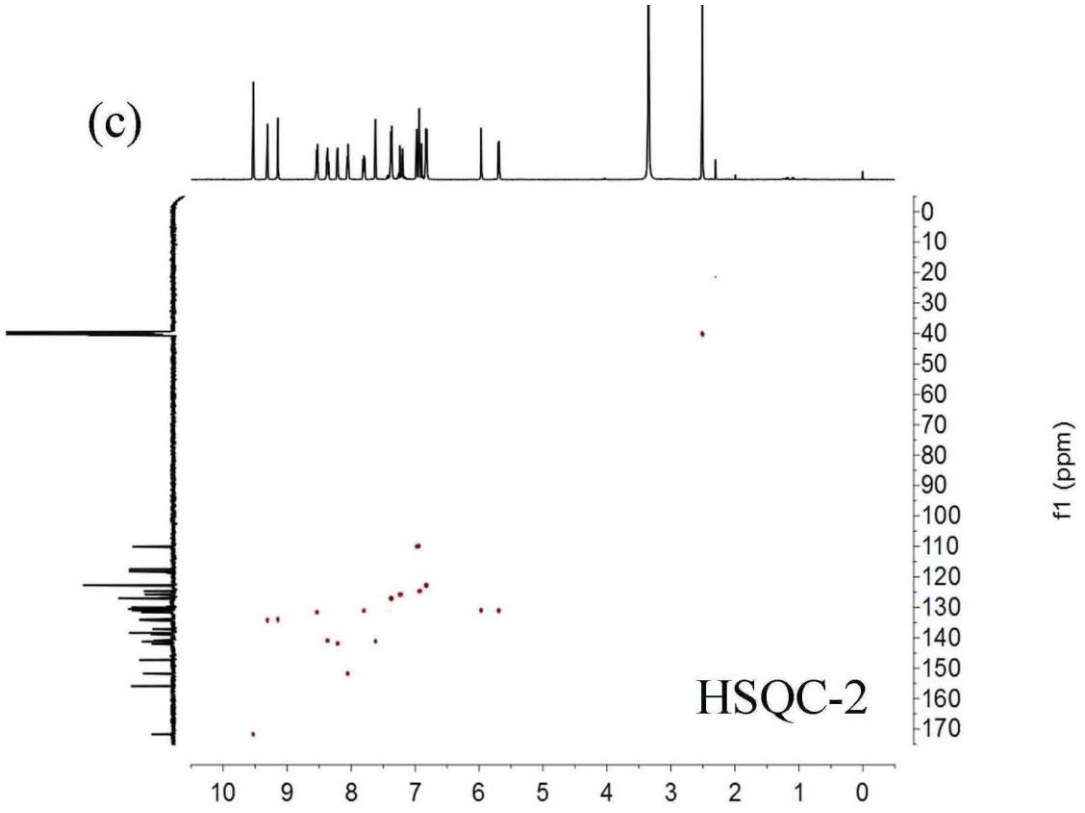


**Fig. S10** (a) 2D COSY NMR spectrum of complex **2** in DMSO-$d_6$. (b) 2D H MBC NMR spectrum of complex **2** in DMSO-$d_6$. (c) 2D HSQC NMR spectru m of complex **2** in DMSO-$d_6$.

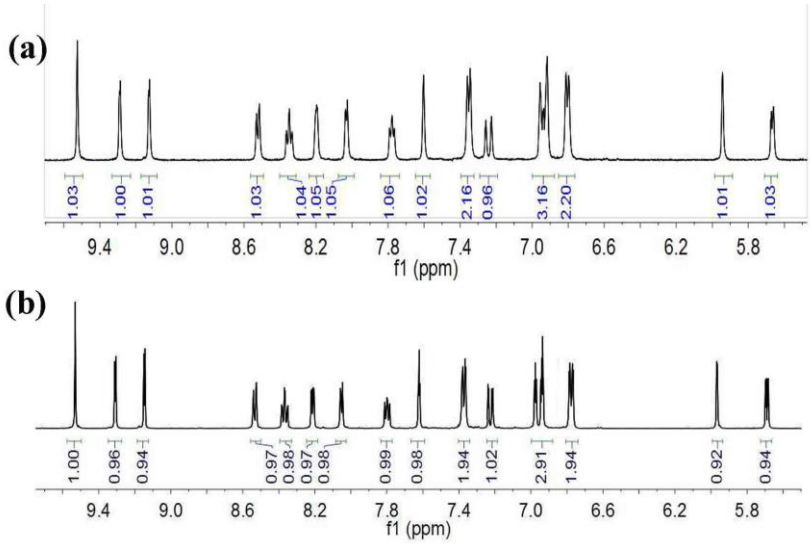


**Fig. S11** Expansion of the aromatic region for complex **2** before grinding (a) and after grinding (b).

## 5. X-ray crystallographic data

The molecular structure of complex **1** was confirmed by X-ray crystallographic analysis of single crystals. Diffraction data were collected on a Bruker SMART Apex CCD diffractometer using k(Mo-K) radiation (k = 0.71073 Å). Cell refinement and data reduction were made by the SAINT program. The structure was determined using the SHELXTL/PC program. Fig. 4 shows Oak Ridge thermal ellipsoid plot (ORTEP) drawings of complex **1**. The crystallographic data have been deposited with the Cambridge Crystallographic Data Centre with CCDC deposition numbers 1046679. These data can be obtained free of charge from The Cambridge Crystallographic Data Centre via www.ccdc.cam.ac.uk/data_request/cif.

**Table S4** Crystal data and structure refinement for complex **1**.

| | Complex **1** |
|---|---|
| Empirical formula | $C_{58}H_{44}F_{20}Ir_2N_{12}OP_2$ |
| Formula weight | 1751.39 |
| Temperature (K) | 293(2) |
| Crystal system | Triclinic |
| space group | P-1 |
| a /Å | 9.382(19) |
| b /Å | 13.771(3) |
| c /Å | 14.966(3) |
| α /° | 63.00(3) |
| β /° | 76.75(3) |
| γ /° | 82.82(3) |
| V/Å$^3$ | 1676.5(6) |
| Z | 1 |
| $\rho_{calc}$ (g/cm$^3$) | 1.735 |
| μ/mm$^{-1}$ | 4.116 |
| $R_{int}$ | 0.0263 |
| Goodness-of-fit on $F^2$ | 0.981 |
| $R_1$[a], $wR_2$[b] [I>2σ(I)] | 0.0489, 0.1359 |
| $R_1$, $wR_2$ (all data) | 0.0648, 0.1425 |

[a] $R_1 = \Sigma||Fo| - |Fc||/\Sigma|Fo|$. [b] $wR_2 = \{ \Sigma[ w( Fo^2 - Fc^2)^2]/ \Sigma[w(Fo^2)^2]\}^{1/2}$

## 6. References


1. (a) G. G. Shan, H. B. Li, Z. C. Mu, D. X. Zhu, Z. M. Su and Y. Liao, *J. Organomet. Chem*., 2012, **702**, 27; (b) E. Baranoff, H. J. Bolink, E. C. Constable, M. Delgado, D. Häussinger, C. E. Housecroft, M. K. Nazeeruddin, M. Neuburger, E. Ortí, G. E. Schneider, D. Tordera, R. M. Walliser and J. A. Zampese, *Dalton Trans.*, 2013, **42**, 1073.
2. M. J. Frisch, G. W. Trucks, H. B. Schlegel, G. E. Scuseria, M. A. Robb, J. R. Cheeseman, G. Scalmani, V. Barone, B. Mennucci, G. A. Petersson, H. Nakatsuji, M. Caricato, X. Li, H. P. Hratchian, A. F. Izmaylov, J. Bloino, G. Zheng, J. L. Sonnenberg, M. Hada, M. Ehara, K. Toyota, R. Fukuda, J. Hasegawa, M. Ishida, T. Nakajima, Y. Honda, O. Kitao, H. Nakai, T. Vreven, J. A. Montgomery, Jr., J. E. Peralta, F. Ogliaro, M. Bearpark, J. J. Heyd, E. Brothers, K. N. Kudin, V. N. Staroverov, R. Kobayashi, J. Normand, K. Raghavachari, A. Rendell, J. C. Burant, S. S. Iyengar, J. Tomasi, M. Cossi, N. Rega, J. M. M. Millam, M. Klene, J. E. K. Knox, J. B. C. Cross, V. Bakken, C. Adamo, J. Jaramillo, R. Gomperts, R. E. Stratmann, O. Yazyev, A. J. Austin, R. Cammi, C. Pomelli, J. W. Ochterski, R. L. Martin, K. Morokuma, V. G. Zakrzewski, G. A. Voth, P. Salvador, J. J. Dannenberg, S. Dapprich, A. D. Daniels, O. Farkas, J. B. Foresman, J. V. Ortiz, J. Cioslowski and D. J. Fox, Gaussian 09, Revision A.02, Gaussian, Inc, Wallingford CT, 2009.